The FASEB Journal

FASEB
Federation of American Societies for Experimental Biology

RESEARCH ARTICLE OPEN ACCESS

Loss of Striatal Bradykinin B2 Receptor Alters Anxiety and Motivational Behaviors in Male Mice

Mariana Rosolen Tavares[1] | Ronaldo Carvalho Araujo[2] | Marina Galleazzo Martins[3] | Jose Donato Jr[3] | Michael Bader[4,5,6] | Frederick Wasinski[1]

[1]Department of Neurology and Neurosurgery, Federal University of Sao Paulo, Sao Paulo, Brazil | [2]Department of Biophysics, Federal University of Sao Paulo, Sao Paulo, Brazil | [3]Department of Physiology and Biophysics, Instituto de Ciencias Biomedicas, Universidade de Sao Paulo, Sao Paulo, Brazil | [4]Max-Delbrück Center for Molecular Medicine (MDC), Berlin, Germany | [5]German Center for Cardiovascular Research (DZHK), Berlin, Germany | [6]Institute for Biology, University of Lübeck, Lübeck, Germany

Correspondence: Frederick Wasinski (f.wasinski@unifesp.br)

Received: 6 March 2026 | **Revised:** 5 May 2026 | **Accepted:** 14 May 2026

Keywords: bradykinin B2 receptor | dorsal striatum | locomotor activity | medium spiny neurons | reward-related behavior

ABSTRACT

The kallikrein–kinin system (KKS) has been extensively studied in peripheral tissues, but its role in the central nervous system (CNS) remains poorly understood. The bradykinin B2 receptor (B2R) is constitutively expressed in the brain, where it may modulate neuronal differentiation, neuroplasticity, and behavioral aspects. Here, we investigated the functional role of striatal B2R by conditionally deleting the *Bdkrb2* gene in the dorsal striatum of adult male mice ($Bdkrb2^{flox/flox}$) using bilateral stereotaxic injections of an AAV8 that induces Cre and tdTomato expression. Mice lacking B2R in the dorsal striatum displayed several context-dependent behavioral alterations, such as reduced anxiety-like behavior and decreased sucrose preference. Moreover, these animals showed enhanced voluntary wheel running, suggesting alterations in motivation-related behavioral output. Immunofluorescence analysis revealed that among dTomato-positive neurons, approximately 17% co-expressed DARPP-32, indicating that a subset of the transduced cells corresponds to dopaminoceptive medium spiny neurons. Together, these findings show that dorsal striatal B2R deletion alters anxiety-related and motivational/hedonic behaviors in male mice and suggest that these effects may involve striatal neuronal populations, including a subset of dopaminoceptive neurons.

1 | Introduction

The kallikrein–kinin system (KKS) is a regulatory cascade involved in multiple physiologic processes, particularly in vascular homeostasis and inflammatory response. It comprises kininogens, kallikreins, kinins, kininases, and kinin receptors, which together act on the vascular system to modulate blood pressure, vascular permeability, and heart rate [1–5]. Kinins are produced in the plasma and peripheral tissues in response to infection, tissue injury, or during inflammatory processes [6]. A significant component in KKS signaling is bradykinin (BK), a nonapeptide generated from kininogens by the action of kallikrein enzymes [7]. BK was first described in 1949 by Brazilian scientists, who identified it as a vasodilatory factor released in the plasma upon exposure to *Bothrops jararaca* venom [8, 9].

Kinins exert their effects through two G-protein coupled receptors: the bradykinin B1 receptor (B1R) and the bradykinin B2 receptor (B2R) [10, 11]. BK and kallidin are high-affinity agonists of B2R, which is constitutively expressed in most tissues under physiological conditions. Kininase I and carboxypeptidase-M remove an arginine residue from the carboxy-terminus

of kinins, generating des-Arg^{9}-BK and des-Arg^{10}-kallidin. These kinin derivatives act as agonists of B1R, which is primarily expressed under stress conditions [7].

The KKS has been extensively studied in peripheral tissues, where it exerts protective effects in the renal and cardiovascular systems [12, 13]. However, KKS dysregulation has been associated with pathological conditions, including diabetic complications, nephropathy [14, 15], retinopathy [16, 17], and cardiovascular disease [18]. Although the peripheral roles of KKS are well documented, accumulating evidence indicates the involvement of the KKS in the central nervous system (CNS), particularly in the context of brain injury and neuroinflammation [7]. Due to its inflammatory profile, B1R contributes to the pathogenesis of neurodegenerative diseases, while B2R seems to be a neuroprotective agent [19]. Studies have also shown a contribution of B2R in neurogenesis and neuronal differentiation [20–24].

Interestingly, global B2R knockout mice exhibit deficits in physical performance [24], further suggesting a role for this receptor in the CNS and behavioral regulation. Our goal was therefore to investigate the physiologic role of B2R in the brain, since this receptor is widely expressed in the mouse cerebral tissue, particularly in the cortex, striatum, and hippocampus [25]. Investigating the localized impact of B2R deletion within discrete brain circuits may provide important insights into its role in CNS function. In this study, we focus on the dorsal striatum, a key structure involved in motor control, cognition, and reward processing [26]. Targeted deletion of the *Bdkrb2* gene in the dorsal striatum was achieved in mice via bilateral stereotaxic injection of an adeno-associated virus (AAV) that induces Cre expression in *Bdkrb2*$^{flox/flox}$ mice.

2 | Materials and Methods

2.1 | Mice

Male *Bdkrb2*$^{flox/flox}$ mice (12–14-week-old) carrying loxP-flanked alleles for the bradykinin B2 receptor gene (*Bdkrb2*) were used in all experiments (The Jackson Laboratory, JAX stock #030446). Animals were homozygous for the floxed *Bdkrb2* alleles and were subjected to stereotaxic injection procedures for regional gene deletion. Genotyping was performed from tail biopsies collected at weaning (3–4 weeks of age) using the REDExtract-N-Amp Tissue PCR Kit (Sigma-Aldrich, St. Louis, Missouri, USA). The presence of the floxed *Bdkrb2* alleles was confirmed by PCR following the supplier's protocol. Mice were housed in standard cages under controlled conditions (12-h light/dark cycle, 22°C ± 2°C, 50%–60% humidity) with ad libitum rodent chow (Nuvilab CR-1, Quimtia, Brazil) and water, unless otherwise specified. All experimental procedures were approved by the Ethics Committee on the Use of Animals of the Universidade Federal de Sao Paulo (Date: 02/10/2023 No: 5501010623).

2.2 | Stereotaxic Surgery

For bilateral injections into the dorsal striatum, *Bdkrb2*$^{flox/flox}$ mice were anesthetized with a ketamine-xylazine cocktail (90 and 13.8 μg/g body weight, respectively, intraperitoneally, IP). After the loss of reflexes, preoperative analgesia was administered with ketoprofen (12 mg/kg; subcutaneous injection). Mice were positioned in a stereotaxic apparatus (Stoelting, Wood Dale, Illinois, USA), and anesthesia was maintained with Isoflurane (2%) throughout the procedure. To induce region-specific deletion of the *Bdkrb2* gene in striatal neurons, an adeno-associated virus (AAV8-hSyn-Cre-P2A-dTomato; Addgene plasmid #107738, Watertown, Massachusetts, USA) was bilaterally injected (800 nL per side; infusion rate: 200 nL/min) using a Hamilton microsyringe (1 μL). Injections were targeted to the dorsal striatum at the following coordinates relative to bregma (according to the Allen Mouse Brain Atlas, https://mouse.brain-map.org/static/atlas) as the reference: +1.00 mm anteroposterior, ±1.70 mm mediolateral, and −3.00 mm depth. Control mice received a bilateral injection of AAV8-hSyn-mCherry (Addgene plasmid #114472). *Bdkrb2*$^{flox/flox}$ mice were randomly assigned to receive either AAV8-hSyn-Cre-P2A-dTomato (ST$^{\Delta B2R}$) or AAV8-hSyn-mCherry (CTL). After injection, the needle was kept in place for 5 min before withdrawal to minimize backflow. The skin was sutured using a sterile nonabsorbable nylon suture 6–0 (Supermedy, Sao Paulo, Brazil). Mice were monitored until they had fully recovered from anesthesia. There was a minimum recovery period of 4 weeks before undergoing behavioral or molecular analyzes. The surgeries were performed in two separate cohorts at different time points. Since injections were variable, only mice in which the dorsal striatum was accurately and bilaterally targeted were included in the ST$^{\Delta B2R}$ group. Viral expression was assessed using reporter fluorescence across serial coronal sections to ensure accurate localization within the dorsal striatum. Targeting accuracy was verified across multiple rostrocaudal sections based on anatomical landmarks. Animals showing unilateral expression or significant off-target spread were excluded from the analysis ($n = 6$ excluded), corresponding to 37.5% of injected animals.

2.3 | Glucose Tolerance Test (GTT)

The glucose tolerance test was performed as previously described [27] in a single cohort of operated animals ($n = 3–6$ per group). Mice were fasted for 4 h during the light phase (from 9:00 a.m. to 1:00 p.m.) with free access to water. Following the fasting period, a glucose solution (2 g/kg of body weight; D-glucose, Sigma-Aldrich, St. Louis, Missouri, USA) was administered intraperitoneally (IP). Blood glucose levels were measured from the tail vein at baseline (0 min) and at 15-, 30-, 60-, 90-, and 120-min postinjection using a handheld glucometer (Accu-Chek Performa, Roche Diagnostics, Mannheim, Germany). Glucose tolerance was evaluated based on the area under the curve (AUC) calculated from individual glucose–time profiles. All measurements were conducted under controlled ambient conditions (22°C ± 1°C, 40%–60% humidity) and by an experimenter blinded to group allocation.

2.4 | Behavioral Assessments

All behavioral assessments were conducted in both cohorts, between 2:00 and 4:00 p.m., to minimize circadian variability, except for voluntary wheel running, which was continuously

monitored over multiple days. Experiments were conducted as previously described [27]. Between trials, all apparatuses were thoroughly cleaned with 20% ethanol and allowed to air dry to eliminate olfactory cues or residues from previous animals. Behavioral sessions were video-recorded, and data were automatically tracked and analyzed using EthoVision XT 17 software (Noldus Information Technology, Wageningen, Netherlands, RRID:SCR_000441). All behavioral assessments were performed in a quiet, dimly lit room, with the experimenter blinded to the experimental groups. Data were analyzed by combining both cohorts. The tests were conducted in the order described in the Methods section, and the intervals are specified within the description of each test. Mice that did not respond to the behavioral tests were excluded from the analyzes.

2.5 | Open Field (OFT) and Elevated Plus Maze Tests (EPM)

Mice were placed in a round open field arena (40 cm [w] × 40 cm [d] × 30 cm [h]) for 5 min to evaluate spontaneous locomotor activity and exploratory behavior. Total distance traveled and the time spent in the center versus the periphery were quantified [27]. The apparatus was made of acrylic and illuminated at 35 lx. Before testing, animals were habituated to the experimental room for at least 30 min to minimize novelty-induced stress. For the elevated plus maze, animals were placed in the center of a maze apparatus elevated 40 cm above the floor, consisting of two opposing open arms (35 cm × 4 cm) and two enclosed arms of identical dimensions. The EPM test was conducted 48 h after the OFT to avoid carry-over effects. The total distance traveled and the time spent in the open versus closed arms were recorded during a 5-min session [27]. A minimum recovery period of 1 week was allowed before conducting the hedonic behavior tests.

2.6 | Hedonic Behavior: Taste and High-Fat Diet Preference Test

The sucrose preference test was used to evaluate hedonic behavior. Mice were first given two bottles of filtered water for 3 days to allow for habituation. After this period, one bottle was replaced with a sucrose solution (0.8 M), while the other continued to contain filtered water, and both were provided for 24 h. To control for side preference, the positions of the bottles were switched halfway through the test. The volume of each solution consumed was then measured [28]. A 72-h washout period was provided between the 24-h sucrose preference test and the high-fat diet preference test, during which animals had ad libitum access to a single bottle of water.

For the high-fat diet (HFD) preference test, mice were simultaneously offered two food sources: standard chow (11.8% kcal fat, 62.6% carbohydrate, 25.6% protein; Nuvilab CR-1, Quimtia) and a high-fat diet (HFD—45% kcal fat, 35% kcal carbohydrate, 20% kcal protein; D12451—Pragsolucoes Biociencias, Jau, Brazil) for 5 days. Containers with the different diets were placed on opposite sides of the cage, and their positions were switched daily to avoid side bias. Body weight and food intake were monitored and recorded daily throughout the testing period [29].

2.7 | Voluntary Wheel Running

Voluntary wheel running assessments were performed after a 1-week recovery period following the high-fat diet preference test, as previously described [27]. Briefly, mice were individually housed in standard cages (30 × 20 × 13 cm) equipped with a freely rotating running wheel with an automatic counter (Commercial Bicycle Computers). The wheels were freely accessible, allowing the animals to engage in voluntary exercise without restriction throughout the duration of the experiment. Wheels were continuously accessible, allowing unrestricted voluntary activity throughout the 7-day experimental period. Running distance was automatically recorded using digital counters, and data were collected daily to quantify spontaneous physical activity levels. Animals that did not access the wheels were excluded from the study. All analyzes were performed by an experimenter blinded to group allocation.

2.8 | Fluorescent in Situ Hybridization

Following the experimental procedures, mice were anesthetized with isoflurane and transcardially perfused with saline, followed by fixation with 10% neutral-buffered formalin. Brains were extracted, postfixed for 1 h in the same fixative, and cryoprotected overnight at 4°C in 0.1 M phosphate-buffered saline (PBS) containing 20% sucrose. Coronal brain sections (30-μm-thick) were obtained using a freezing microtome (SM2010 R Leica Microsystems, Wetzlar, Germany). Coronal sections of the dorsal striatum were submitted to an RNAscope multiplex fluorescent V2 assay (Cat#323110, ACDBio, Newark, California, USA) according to the manufacturer's instructions, followed by an immunofluorescence to detect mCherry-expressing cells. Briefly, sections were rinsed in PBS, dried at 60°C for 30 min, and dehydrated in ethanol. After incubation in H_2O_2 for 10 min at room temperature and Protease III for 30 min at 40°C, sections were incubated with *Bdkrb2* mRNA probe (Mm-*Bdkrb2*, Cat#424351, ACDBio) for 2 h at 40°C. The *Bdkrb2* mRNA was visualized with TSA Plus Fluorescein (1:1500, Cat#NEL741001KT, Akoya Biosciences, Marlborough, Massachusetts, USA). Immediately after, sections were incubated in a primary antibody anti-mCherry made in chicken (1:1000, Cat#mcherry-0100, Aves Labs) for 90 min at 37°C, followed by incubation in Alexa Fluor 594-anti-chicken antibody made in donkey (1:500, Cat #703-586-155, Jackson ImmunoResearch) for 60 min at 25°C. Finally, slides were counterstained with DAPI, cover-slipped with ProLong Gold antifade media (#P36930, ThermoFisher Scientific), and stored in the dark at 4°C until imaging.

2.9 | Image Analysis

To evaluate the potential astrocytic involvement at the injection site and assess neuronal co-localization, immunofluorescence

staining was performed. Since dTomato and mCherry reporter proteins emit native fluorescence, no additional staining was required. Fluorescent images were acquired using an AxioImager A1 microscope (Carl Zeiss, Germany) equipped with an Axiocam 512 camera. Free-floating sections were rinsed in 0.02 M potassium PBS, pH 7.4 (KPBS) and blocked in 3% normal serum for 1 h, followed by overnight incubation in the following antibodies: anti-GFAP (1:1000 Abcam, Waltham, MA; Cat#AB68428), anti-parvalbumin (1:1000 Sigma Aldrich, Saint Louis, Missouri, USA; Cat#P3088), and anti-DARPP-32 (1:1000 Invitrogen, Waltham, Massachusetts, USA; Cat#PA5-85788). In the following step, sections were rinsed in KPBS and incubated for 90 min in Alexa Fluor-conjugated secondary antibodies (1:500, Jackson ImmunoResearch Laboratories, Cambridge, Massachusetts, USA). After rinsing in KPBS, sections were mounted onto gelatin-coated slides and covered with Fluoroshield with DAPI (Sigma-Aldrich, Saint Louis, Missouri, USA; Cat#F6057). For quantification, DARPP-32-positive and double-labeled cells were manually counted at 100× magnification photomicrographs using ImageJ software (RRID:SCR_003070). The mean of five representative coronal sections per hemisphere was obtained for each animal ($n = 4$). Photoshop 2023 (Adobe Inc.) was used to adjust image brightness and contrast, as well as to integrate graphs and digital images into composite figures.

2.10 | Statistical Analysis

Data normality was analyzed using the Shapiro–Wilk test, and homogeneity of variances was assessed prior to selecting parametric tests. For datasets following a normal distribution, two-way repeated-measure ANOVA was used to analyze changes over time, and an unpaired two-tailed Student's *t*-test was used to analyze possible differences between the experimental groups. When significant differences were detected, Sidak's and Tukey's post hoc analyzes were conducted to identify pairwise differences. In cases of nonnormal distribution, the nonparametric Mann–Whitney test was applied. Results are expressed as mean ± standard error of the mean (SEM), and statistical significance was defined as $p < 0.05$. All bar graphs display individual data points overlaid on the bars. All statistical analyzes were carried out using GraphPad Prism software, version 8.0.1 (GraphPad Software, San Diego, California, USA, RRID:SCR_002798). Detailed information on statistical tests, degrees of freedom, and sample sizes for each experiment is provided in Table S1.

3 | Results

3.1 | Striatal B2R Deletion via Bilateral Stereotaxic Injections of AAV-Cre

To investigate the role of constitutive B2R expression in dorsal striatal neurons, we conditionally deleted the *Bdkrb2* gene in this region using the Cre-LoxP recombination system. Subsequently, mice were subjected to a series of behavioral and physiological assessments. AAV8-hSyn-Cre-P2A-dTomato was bilaterally injected into the dorsal striatum of *Bdkrb2*$^{flox/flox}$ mice (Figure 1A,B) while *Bdkrb2*$^{flox/flox}$ mice injected with AAV8-hSyn-mCherry served as controls (Figure 1C,D). As shown in Figures 1A–D, the distinct expression patterns of mCherry and dTomato confirmed that B2R expression is restricted to specific neuronal populations within the dorsal striatum. Only mice in which the dorsal striatum was accurately and bilaterally targeted were included in the ST$^{\Delta B2R}$ group.

To confirm the selective deletion of *Bdkrb2* following AAV-Cre-dTomato administration, RNA in situ hybridization was performed to evaluate *Bdkrb2* mRNA expression in virus-transduced dorsal striatum neurons. As shown in Figure 2, *Bdkrb2* mRNA signals (green grains) were detected in the dorsal striatum of control animals, including in mCherry-expressing neurons (left panel, white arrows). In contrast, *Bdkrb2* mRNA staining was practically absent in AAV-Cre-dTomato–transduced striatal neurons (ST$^{\Delta B2R}$ mice, right panel). Thus, the genetic ablation of B2R was successfully accomplished in striatal infected neurons.

3.2 | Striatal B2R Deletion Does Not Affect Body Weight or Glucose Homeostasis

To assess potential metabolic alterations associated with striatal B2R deletion, we analyzed key parameters of metabolic regulation. The absence of B2R signaling in the dorsal striatum did not affect body weight following postsurgical recovery (Figure 3A,B). No major differences in glucose tolerance were detected between groups under the experimental conditions used (Figure 3C,D). However, given the limited sample size used in this analysis, this finding is considered exploratory, and additional studies with larger cohorts will be necessary to determine whether striatal B2R deletion affects metabolic parameters.

3.3 | B2R Ablation in Striatal Neurons Alters Hedonic Behavior Associated With Sucrose Consumption

Hedonic behavior was evaluated using preference tests for both a high-fat diet (HFD) and sucrose. During the HFD preference test, food intake of standard chow and HFD was measured over 5 days. Both groups showed a greater preference for the HFD compared with standard chow, even though ST$^{\Delta B2R}$ mice exhibited a transiently higher HFD intake on Day 1 relative to controls (Figure 4A). However, this difference was no longer observed in the subsequent days. As expected, body weight increased progressively during the 5-day intervention, with no significant differences between groups (Figure 4B).

In the sucrose preference test, animals were presented with two bottles for 24 h, one containing filtered water and the other a 0.8 M sucrose solution. Compared with controls, ST$^{\Delta B2R}$ mice showed a marked reduction in sucrose consumption (Figure 4C), indicating decreased sucrose preference, which may reflect alterations in hedonic and/or motivational processing. Body weight remained similar between groups throughout the testing period (Figure 4D).

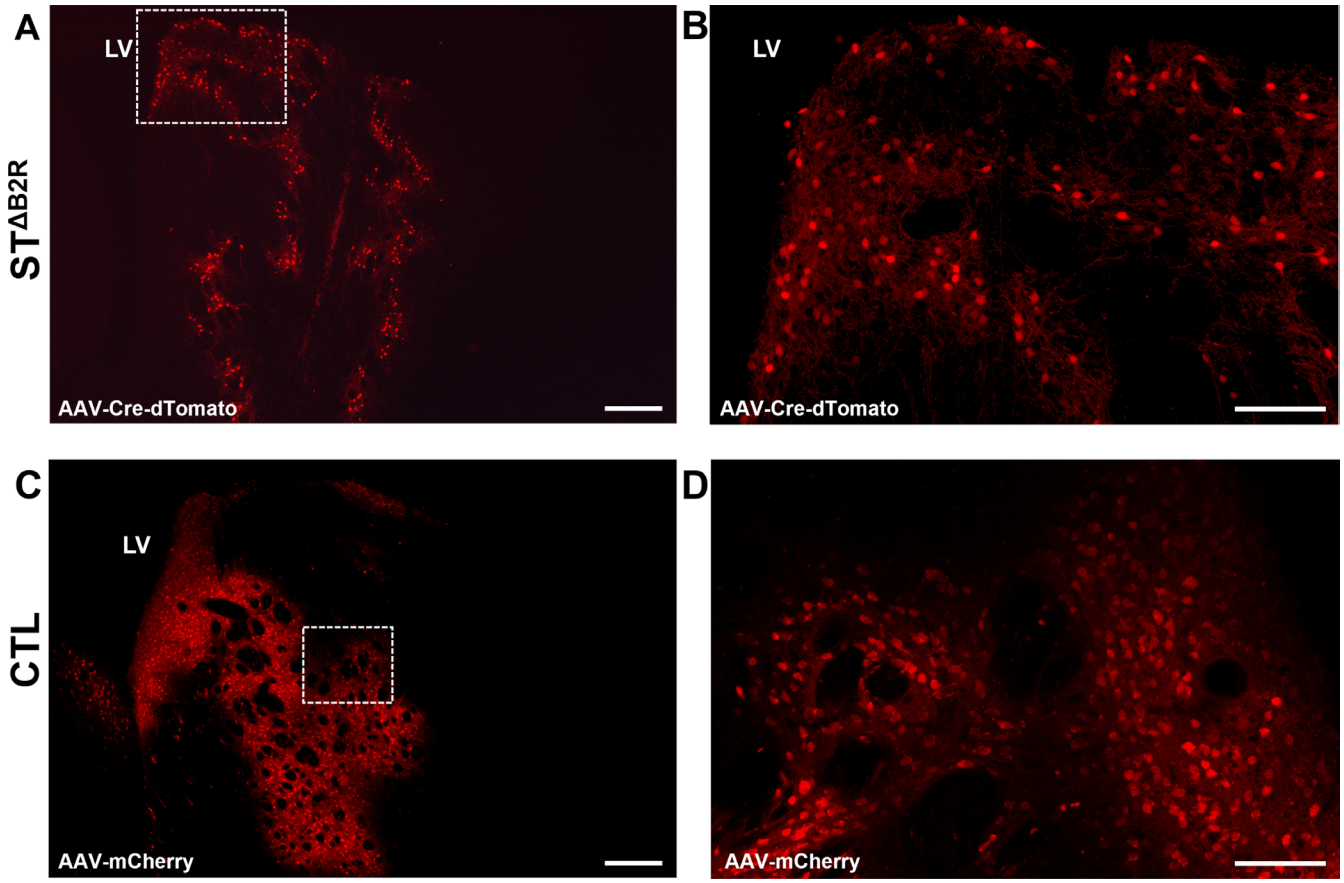

FIGURE 1 | Bilateral AAV injections into the dorsal striatum to delete bradykinin B2 receptor (B2R) from striatal neurons. (A, B) Representative fluorescence images of AAV-Cre-dTomato expression in the dorsal striatum (ST$^{\Delta B2R}$ mice). (C, D) Representative fluorescence images showing AAV-mCherry expression in the control (CTL) group in the dorsal striatum. $n = 10–12$ per group. Scale bar: 50 μm (left panels) and 100 μm (right panels). LV: Lateral ventricle.

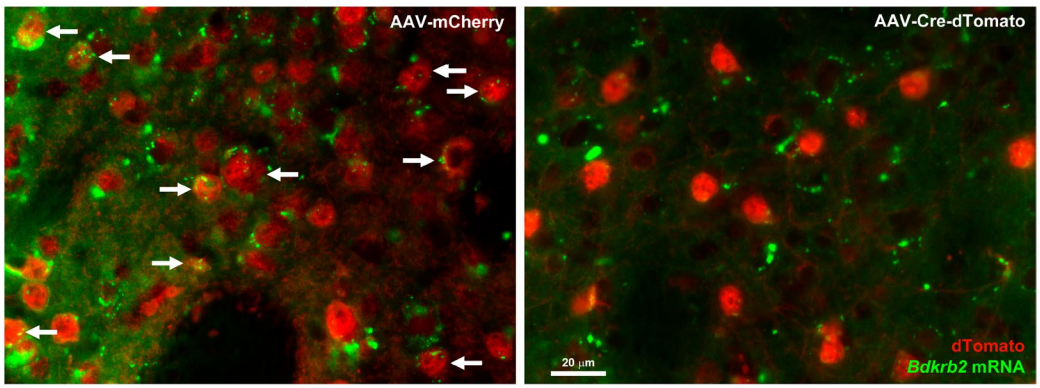

FIGURE 2 | Targeted deletion of the B2R from dorsal striatal neurons. RNA in situ hybridization showing the presence of *Bdkrb2* mRNA (green staining) in striatal neurons from AAV-mCherry (control) injected mice (left panel, white arrows) and the absence of *Bdkrb2* mRNA in striatal neurons from AAV-Cre-dTomato (ST$^{\Delta B2R}$) injected mice. $n = 3$ per group. Scale bar: 20 μm.

3.4 | Loss of B2R Signaling in Striatal Neurons Attenuates Anxiety-Like Behavior and Enhances Voluntary Physical Activity

Behavioral assays were conducted to evaluate anxiety-related responses and locomotor activity. In the open field test, no significant differences were observed between groups in the time spent in the central or peripheral zones or in the total distance traveled (Figures 5A–C), indicating preserved baseline locomotion and exploratory behavior. In contrast, in the elevated plus maze, ST$^{\Delta B2R}$ mice spent more time in the open arms compared to controls (Figures 5E–F), suggesting reduced context-dependent anxiety-like behavior. Total distance traveled did not differ between groups (Figure 5A,D), confirming that locomotor performance remained unaltered.

Over the course of 7 days of voluntary wheel running, ST$^{\Delta B2R}$ mice exhibited greater daily running distances than controls

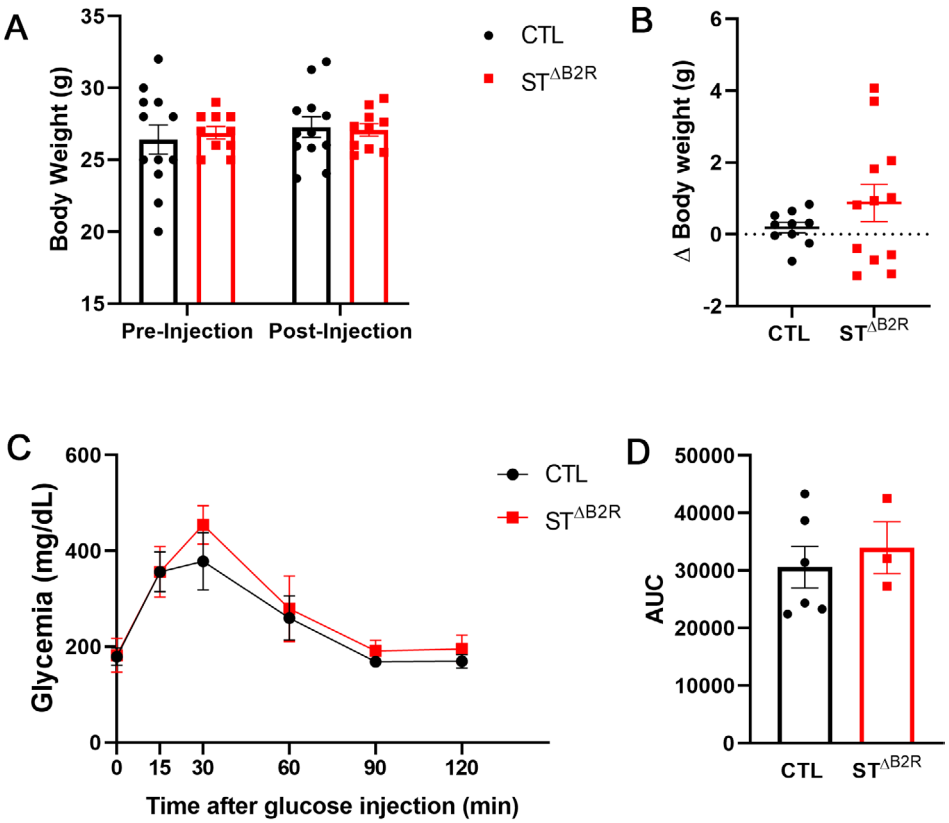

FIGURE 3 | Striatal B2R ablation does not affect body weight or glucose tolerance. (A, B) Body weight measured before and after viral injection and the corresponding body weight change in control (CTL) and $ST^{\Delta B2R}$ mice ($n = 10–12$ per group). (C, D) Glucose tolerance test (GTT) curve and area under the curve (AUC) for CTL and $ST^{\Delta B2R}$ groups ($n = 3–6$ per group). Data are expressed as mean ± SEM.

(Figure S2), resulting in a higher cumulative distance from the third day onwards (Figure 6). These findings suggest that striatal B2R signaling may modulate emotional and motivational circuits underlying both anxiety and spontaneous physical activity.

3.5 | A Subset of Striatal B2R-Expressing Neurons Colocalizes With Dopaminoceptive Neurons

Because the AAV used in this study does not target a specific neuron type, we next sought to identify the neuronal populations potentially affected by B2R deletion in the striatum. Immunofluorescence analyzes were performed to determine whether the AAV driving Cre expression (expressing dTomato) colocalized with markers of specific striatal cell types, given that specific antibodies for kinin receptors are not currently available. Immunofluorescence analysis revealed no colocalization of the reporter (dTomato) with GFAP (Figure S3A) or parvalbumin (Figure S3B), excluding viral transduction in astrocytes and striatal interneurons.

Analysis of DARPP-32 expression, a key CNS protein that mediates dopamine signaling and serves as a major marker of dopaminoceptive medium spiny neurons [30], revealed that among the neurons affected by the viral injection, 17.5% of them expressed DARPP-32 (Figure 7A–G). This finding suggests that a subset of the transduced neurons corresponds to dopaminoceptive medium spiny neurons; however, the precise identity of most transduced cells remains undefined.

4 | Discussion

In this study, we investigated the physiological role of B2R in the mouse dorsal striatum using the Cre-LoxP system to selectively delete B2R from striatal neurons. The use of viral vectors for stereotaxic region-specific gene ablation provides important advantages over traditional knockout models. This strategy provides a cleaner and more physiologically confined manipulation compared to constitutive knockout models [31]. In global B1R or B2R knockout animals, compensatory cross-regulation is frequently observed, where the absence of one receptor induces overexpression or enhanced activity of the other, thereby masking receptor-specific effects [32]. Moreover, conventional Cre-driver line strategies often introduce confounding factors such as germline recombination, mosaic Cre activity, and ectopic expression, which can compromise regional specificity. These phenomena typically result from Cre expression in germ cells, parental sex bias, and locus-dependent variability, leading to unwanted global deletions or inter-individual heterogeneity in recombination efficiency [33]. Therefore, striatal B2R deletion achieved through localized AAV-Cre injection minimizes both systemic compensatory adaptations and germline-related artifacts, allowing a more direct assessment of B2R functions in the striatum.

To further ensure neuronal specificity, we employed a Cre construct under the control of the neuron-specific *hSyn* promoter, thereby avoiding off-target expression in glial populations. Injection sites were verified by dTomato fluorescence across

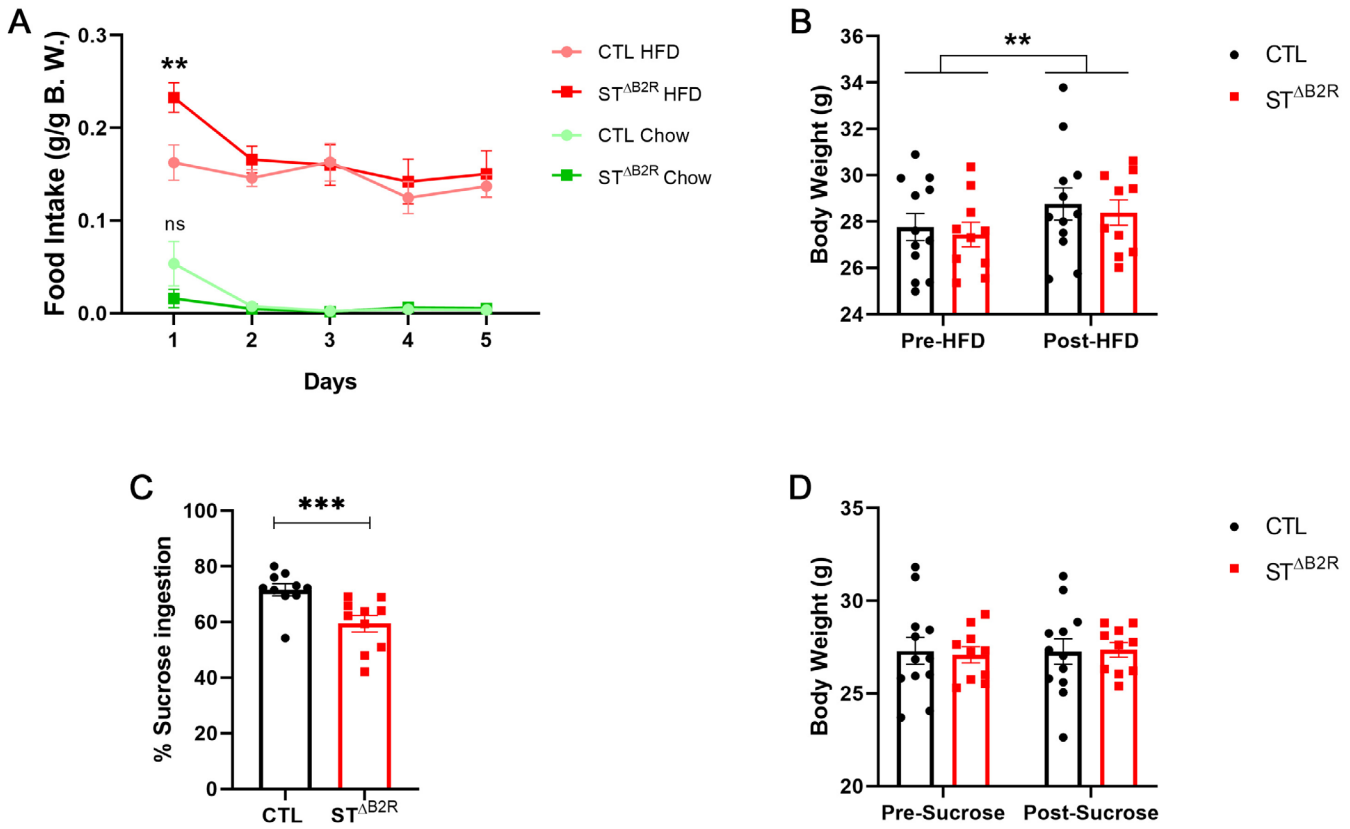

FIGURE 4 | Striatal B2R deletion modifies hedonic behavior in the sucrose preference test. (A) Daily intake of standard chow and high-fat diet (HFD) across 5 days; (B) Change in body weight following the dietary intervention; (C) Sucrose consumption over a 24-h period; (D) Body weight change after the sucrose preference test in control (CTL) and $ST^{\Delta B2R}$ mice ($n = 10$ per group). Data are expressed as mean ± SEM. Statistical significance was assessed using Two-way ANOVA followed by Tukey's or Sidak's multiple comparisons tests; or the Mann–Whitney *U*-test where appropriate; $^{**}p < 0.01$; $^{***}p < 0.001$. NS, not significant.

serial coronal sections encompassing the dorsolateral and dorsomedial regions of the striatum. Although viral targeting was restricted to the dorsal striatum based on anatomical verification, viral spread to adjacent regions such as the nucleus accumbens or cortex was not quantitatively assessed. Therefore, potential off-target effects cannot be fully ruled out. The AAV's efficacy in deleting *Bdkrb2* mRNA was confirmed by RNA in situ hybridization, providing qualitative validation of recombination in transduced neurons, as no specific antibody for B2R is currently available. This targeted approach complements previous studies from our group using $TH^{\Delta B2R}$ mice, providing a more restricted manipulation that isolates the contribution of striatal B2R from broader dopaminergic circuitry effects.

Previous studies have suggested a role for B2R in motor control [24] and have reported its potential dimerization with the dopamine D2 receptor (DrD2) under in vitro conditions [34]. Given that the dorsal striatum receives dopaminergic projections from the substantia nigra pars compacta and abundantly expresses DrD2 [35], this region represents a particularly relevant site to investigate the contribution of B2R to sensorimotor regulation. In addition to its role in motor circuits, dopaminergic signaling within the striatum also modulates behaviors related to motivation, reward, and hedonic processing [36].

Classical studies have established a strong association between the nucleus accumbens (NAc) of the ventral striatum and reward-related behaviors [35], whereas the dorsal striatum is traditionally associated with motor coordination and goal-directed action selection. However, a pivotal study demonstrated that the dorsal striatum also contributes to reward and motivation, particularly by modulating feeding behavior [37]. $ST^{\Delta B2R}$ mice exhibited a transient increase in HFD intake compared with controls during the initial day of exposure; however, this effect was not sustained in subsequent sessions (Figure 4A). Such early hyperphagic responses are often reported in rodents following the introduction of palatable diets and are typically mediated by hypothalamic orexigenic mechanisms involving AgRP/NPY-expressing neurons [38]. Therefore, the transient hyperphagic effect likely reflects an acute novelty or palatability-driven response rather than a persistent alteration in reward valuation or energy balance.

Several studies have demonstrated that experimental conditions, including stress exposure, deprivation schedules, and circadian timing, can significantly influence sucrose preference outcomes [39, 40]. In our study, mice were acclimated to the two-bottle setup for three consecutive days, and testing was performed under baseline physiological conditions, without additional stressors such as food or water restriction. Under these conditions, $ST^{\Delta B2R}$ mice exhibited a reduced sucrose preference (Figure 4C). Normalizing sucrose intake to body weight attenuated but did not abolish the group difference ($p = 0.0005$ vs. $p = 0.0108$; Figure S1), reinforcing that the effect was not solely attributable to body mass variability.

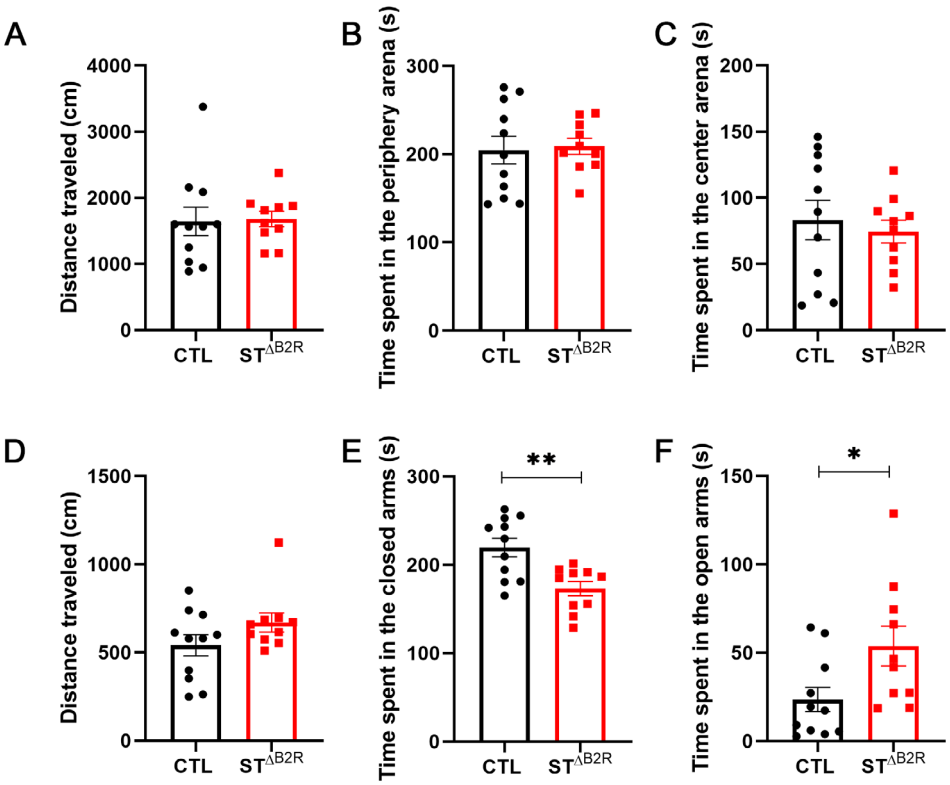

FIGURE 5 | Striatal B2R deletion modulates anxiety-like behavior without affecting locomotion. (A–C) Total distance traveled, time spent in the periphery, and time spent in the center of the open-field arena; (D–F) Total distance traveled, time spent in the closed arms, and time spent in the open arms of the elevated plus maze in control (CTL) and ST$^{\Delta B2R}$ mice ($n = 10–11$ per group). Data are expressed as mean ± SEM. Statistical significance was determined by Student's *t*-test; $^{*}p < 0.05$; $^{**}p < 0.01$.

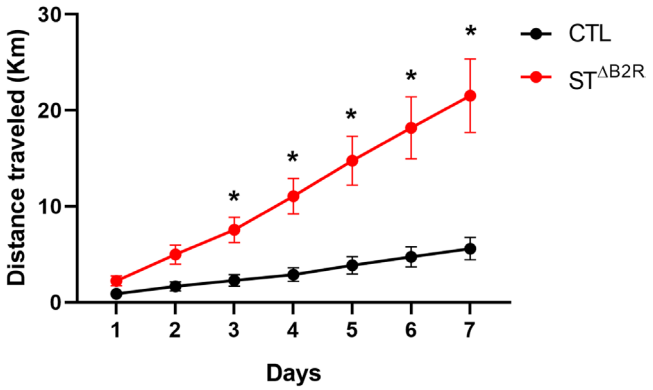

FIGURE 6 | Striatal B2R deletion enhances voluntary wheel-running activity. Cumulative running distance (in kilometers) recorded over the seven consecutive days period in control (CTL) and ST$^{\Delta B2R}$ mice ($n = 7–10$ per group). Data are expressed as mean ± SEM. Statistical analysis was performed using two-way repeated-measures ANOVA followed by Sidak's multiple comparisons test. $^{*}p < 0.05$.

Anhedonia remains a multifaceted construct in animal models, typically divided into motivational and consummatory components. The sucrose preference test primarily captures the consummatory aspect, as it requires minimal effort for reward acquisition [39]. In our study, ST$^{\Delta B2R}$ mice did not display altered consummatory behavior toward either standard chow or high-fat diets (Figure 4A), suggesting that the observed decrease in sucrose preference does not reflect a generalized reduction in hedonic drive. Moreover, we did not assess orofacial responses or licking frequency, measures that could have provided a more nuanced evaluation of anhedonia [41]. Therefore, the observed reduction in sucrose preference cannot be interpreted as a definitive measure of anhedonia. Additionally, because B2R is expressed in peripheral sensory neurons, we cannot exclude the possibility that changes in gustatory processing contribute to this phenotype. Future studies incorporating detailed behavioral analyzes will be required to clarify these mechanisms.

In contrast, anxiety-like behavioral assays, including the open field and elevated plus maze [41, 42], did not reveal heightened anxiety in ST$^{\Delta B2R}$ mice (Figure 5B,C,E,F). Interestingly, these animals spent more time in the open arms, indicative of task-specific reduced anxiety-like behavior compared with controls [41] (Figure 5E), which may reflect alterations in neural circuits modulated by B2R within the striatum. Although both the open field test and the elevated plus maze are commonly used to assess anxiety-like behavior, they rely on distinct behavioral paradigms. The open field test primarily assesses exploratory behavior and avoidance of the center of an open arena, whereas the elevated plus maze introduces an additional conflict—elevated spaces—between exploration and the aversion to open arms, making it a more robust measure for detecting a specific anxiety-like phenotype [43]. In the present study, the absence of differences in the open field test, together with increased open arm exploration in the elevated plus maze test, suggests a context-dependent modulation of anxiety-related behavior rather than a generalized anxiolytic phenotype.

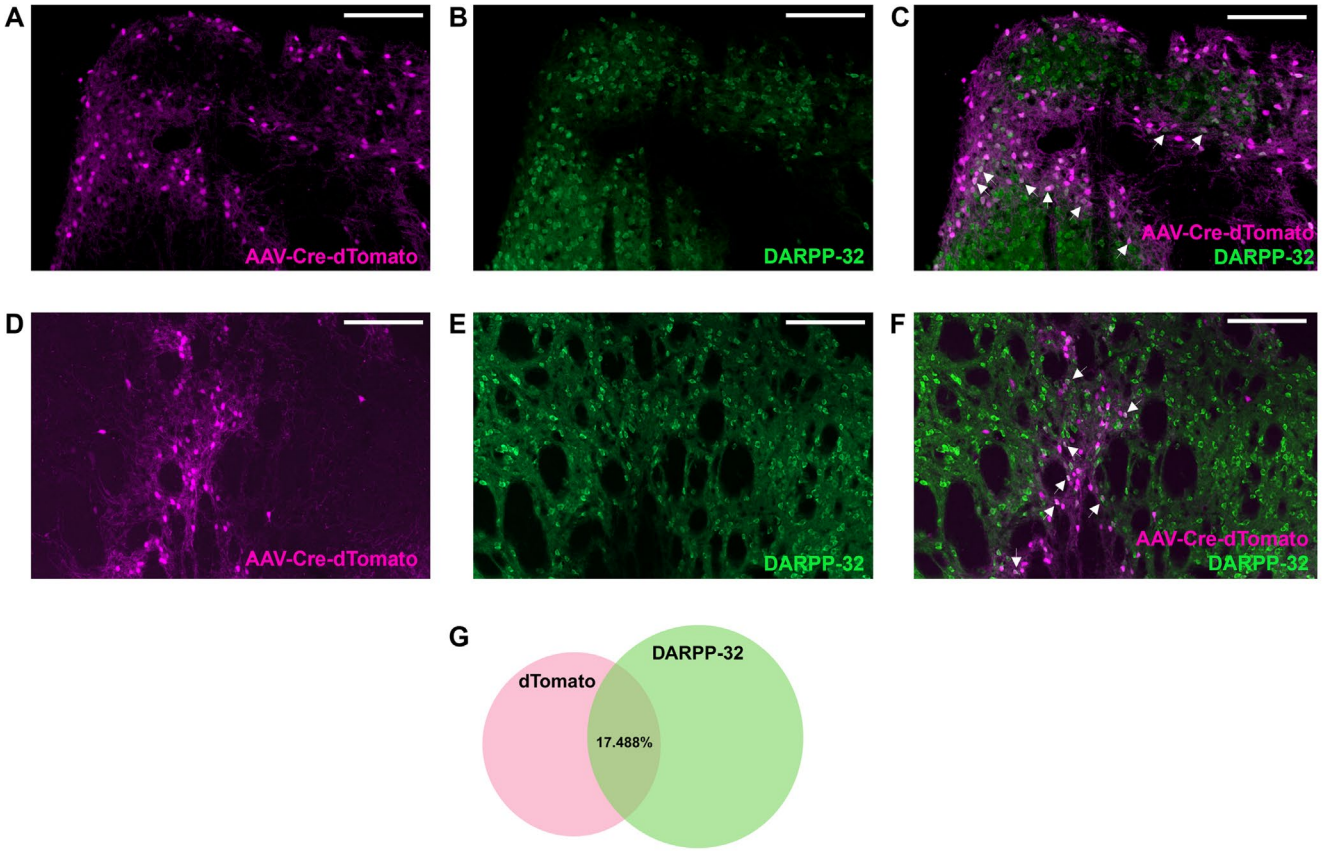

FIGURE 7 | Co-localization of dTomato reporter expression with DARPP-32-positive neurons in the dorsal striatum. (A, D) Representative immunofluorescence micrographs showing dTomato reporter expression (magenta); (B, E) Representative immunofluorescence micrographs showing DARPP-32 labeling (green); (C, F) Representative immunofluorescence micrographs showing dTomato and DARPP-32 co-localization of $ST^{\Delta B2R}$ mice. White arrows indicate co-localization cells. (G) Schematic representation summarizing the proportion and spatial distribution of dTomato/DARPP-32 co-localized neurons ($n = 4$). Scale bar: 200 μm. LV: Lateral ventricle.

Voluntary wheel running can influence performance in subsequent behavioral assays, including sucrose preference, high-fat diet intake, and anxiety-related tests such as the open field and elevated plus maze [44–46]. To minimize potential *carryover* effects, we adopted a fixed testing order and implemented sufficient inter-test intervals, ensuring that the observed outcomes reflected true behavioral phenotypes rather than procedural artifacts—even if the presentation of results in this manuscript does not strictly follow the chronological testing sequence.

Classical motor control within the dorsal striatum involves two principal pathways: the direct pathway, facilitated by dopamine D1 receptor (DrD1) activation, which promotes movement initiation, and the indirect pathway, driven by DrD2 activation, which suppresses movement [47, 48]. Although these canonical models have been extensively studied, experimental manipulations targeting DrD1 and DrD2 expressing neurons in the dorsal striatum can produce divergent effects on locomotor output [49]. Similarly, selective activation of DrD1 and DrD2 neurons in the ventral striatum's nucleus accumbens produces opposing effects on locomotion and running behavior [36].

In our study, striatal B2R ablation did not affect locomotor activity in aversive assays such as the open field and elevated plus maze (Figure 5A,D). In contrast, when animals were exposed to a rewarding stimulus—voluntary wheel running [44, 50]—mice lacking striatal B2R showed increased running activity, except during the first 2 days, which are typically considered an acclimation or habituation phase (Figure 6). Interestingly, daily analysis revealed that $ST^{\Delta B2R}$ mice already exhibited greater distances traveled from the very first day (Figure S2). Voluntary wheel-running in rodents is a complex behavior output influenced by motivation and hedonic drives, sensitivity to stress, and activation of mesolimbic dopaminergic circuits [44]. Given that experiments were performed under physiological conditions without additional stressors or inflammatory stimuli, the enhanced running behavior observed in $ST^{\Delta B2R}$ mice may reflect alterations in reward-related processing or motivational components, potentially involving modulation of striatal circuits. Future studies investigating dopaminergic signaling markers, such as tyrosine hydroxylase (TH) or DARPP-32 phosphorylation, may clarify the mechanistic basis of this enhanced motivational behavior.

At first glance, the combination of reduced sucrose preference and increased voluntary wheel running may seem paradoxical. However, these behaviors reflect distinct components of reward processing. The sucrose preference test primarily measures consummatory aspects of reward, requiring minimal effort, whereas voluntary wheel running is a more complex behavior involving motivational drive, reinforcement, and goal-directed activity. Thus, the observed phenotype may reflect a dissociation between consummatory and motivational components of reward, rather

than a uniform change in reward sensitivity. Similar dissociations have been reported in other experimental contexts, underscoring the multifaceted nature of reward-related behaviors. These findings further support the notion that reward is not a unitary construct but comprises multiple dissociable processes that can be independently modulated by specific neural circuits.

This interpretation is consistent with the "liking" versus "wanting" framework proposed by Berridge and colleagues, in which reward-related behavior is divided into dissociable components, including hedonic impact ("liking") and incentive motivation ("wanting"). Within this framework, reduced sucrose preference may reflect alterations in consummatory or hedonic-related processing, whereas increased voluntary wheel running may indicate alterations in motivational drive or incentive-related processes. Therefore, the behavioral profile observed in $ST^{\Delta B2R}$ mice should not be interpreted as a uniform increase or decrease in reward sensitivity, but rather as a dissociation between distinct reward-related domains [51, 52].

The present study was conducted in male mice, which represents a limitation. Sex differences have been widely reported in both kallikrein–kinin system regulation and in reward-related neural circuits and behaviors. Therefore, the extent to which our findings generalize to female animals remains unknown. Considering the known influence of sex hormones on both inflammatory signaling and dopaminergic function, sex-dependent effects of B2R signaling in the brain are a relevant question for future investigation.

Analysis of striatal neuron identity revealed that 17.5% of AAV-Cre-dTomato–transduced neurons expressed DARPP-32 (Figure 7C,F). DARPP-32 is a striatal protein integrating dopaminergic signals via both DrD1 and DrD2 [53]. Over half of DARPP-32–positive neurons co-localize with DrD1 and project to the substantia nigra pars reticulata, forming the direct pathway, whereas the remainder project to the globus pallidus and are characterized by DrD2 and A2A receptor expression, corresponding to the indirect pathways [53–55]. Moreover, evidence suggests that a subset of striatal projection neurons co-expresses both DrD1 and DrD2 [56], underscoring the cellular heterogeneity and functional complexity of basal ganglia output circuits. Notably, this neuronal heterogeneity may contribute to the behavioral outcomes observed in $ST^{\Delta B2R}$ mice, as dual DrD1/DrD2-expressing neurons are proposed to integrate motivational and reward-related signaling.

DARPP-32 does not differentiate between DrD1- and DrD2-expressing medium spiny neurons, which have distinct and often opposing roles in striatal function. Consequently, the precise neuronal identity of most transduced cells remains unclear. This limitation constrains the interpretation of our behavioral findings in terms of specific striatal pathways. Future studies employing cell type–specific approaches—such as RNAscope or multiplex immunofluorescence targeting DrD1, DrD2, and Chat, will be required to define the neuronal populations involved.

However, because a subset of transduced neurons co-expressed DARPP-32, it is possible that part of the observed behavioral phenotype involves dopaminoceptive striatal neurons. Nevertheless, the present study did not directly assess dopamine signaling, and therefore any mechanistic link to dopaminergic transmission remains speculative. Future studies evaluating dopamine content, tyrosine hydroxylase expression, and DARPP-32 phosphorylation will be necessary to determine whether B2R deletion directly affects dopaminergic signaling in the striatum. Importantly, the behavioral findings reported here do not depend on the precise identification of specific striatal neuronal subtypes.

While global B2R knockout has been shown to reduce voluntary wheel-running performance in mice [24], our findings suggest that striatal B2R deletion modulates motor and motivational behaviors in a region and cell-type-specific manner. This effect may involve striatal neuronal populations, including dopaminoceptive neurons, consistent with the established roles of DrD1- and DrD2-mediated pathways in regulating striatal sensorimotor and motivational output [36, 49]. Given that DrD1- and DrD2-expressing neurons exert opposing influences on basal ganglia circuits, it is conceivable that B2R signaling may influence striatal circuits involved in behavioral responses to rewarding stimuli. Although the precise cellular mechanisms and the specific striatal population responsible for the observed effects remain to be elucidated, our results highlight a previously underappreciated role of dorsal striatal B2R in regulating anxiety-related and motivational behaviors. These findings also open new perspectives for exploring kinin receptor–dopamine receptor interactions in neurobehavioral regulation. However, the precise cellular and molecular mechanisms underlying these effects remain to be determined.

Author Contributions

All authors had full access to all the data in the study and take responsibility for the integrity of the data and the accuracy of the data analysis. **M.R.T.** and **F.W.:** conceptualization. **M.R.T.**, **J.D.**, and **F.W.:** methodology. **M.R.T.** and **F.W.:** formal analysis. **M.R.T.** and **F.W.:** validation. **M.R.T.**, and **M.G.M.:** investigation. **F.W.:** resources. **F.W.:** data curation. **M.R.T.** and **F.W.:** writing – original draft preparation. **M.R.T.**, **R.C.A.**, **M.G.M.**, **J.D.**, and **M.B.:** writing – review and editing. **M.R.T.** and **F.W.:** visualization. **F.W.:** supervision. **F.W.:** project administration. **F.W.:** funding acquisition. All authors have read and agreed to the published version of the manuscript.

Acknowledgments

The Article Processing Charge for the publication of this research was funded by the Coordenação de Aperfeiçoamento de Pessoal de Nível Superior - Brasil (CAPES) (ROR identifier: 00x0ma614).

Funding

This research was supported by the Fundação de Amparo a Pesquisa do Estado de São Paulo (FAPESP/Brazil, grant numbers 2019/07005-4 and 2023/01250-2 for F.W.; 2023/09878-0 for M.R.T.; 2024/21641-9 for J.D.); Conselho Nacional de Desenvolvimento Cientifico e Tecnologico (CNPq/Brazil; finance code 151318/2023-9 for M.R.T) and Coordenação de Aperfeiçoamento de Pessoal de Nível Superior (CAPES/PROBRAL; finance code 88881.895020/2023 for R.C.A. and M.B. and CAPES/PRINT; finance code 88887.979375/2024-00 for F.W.).

Ethics Statement

All experimental procedures were approved by the Ethics Committee on the Use of Animals of the Universidade Federal de Sao Paulo (Date: 02/10/2023 No: 5501010623).

Conflicts of Interest

The authors declare no conflicts of interest.

Data Availability Statement

The data that support the findings of this study are available in the Supporting Information of this article.

References

1. P. D. Cherry, R. F. Furchgott, J. V. Zawadzki, and D. Jothianandan, "Role of Endothelial Cells in Relaxation of Isolated Arteries by Bradykinin," *Proceedings of the National Academy of Sciences of the United States of America* 79, no. 6 (1982): 2106–2110.

2. C. Ribuot, D. Godin, R. Couture, D. Regoli, and R. Nadeau, "In Vivo B2-Receptor-Mediated Negative Chronotropic Effect of Bradykinin in Canine Sinus Node," *American Journal of Physiology* 265, no. pt. 2 (1993): H876–H879.

3. P. Meneton, M. Bloch-Faure, A. A. Hagege, et al., "Cardiovascular Abnormalities With Normal Blood Pressure in Tissue Kallikrein-Deficient Mice," *Proceedings of the National Academy of Sciences of the United States of America* 98, no. 5 (2001): 2634–2639.

4. R. H. Ritchie, J. D. Marsh, W. D. Lancaster, C. A. Diglio, and R. J. Schiebinger, "Bradykinin Blocks Angiotensin II-Induced Hypertrophy in the Presence of Endothelial Cells," *Hypertension* 31, no. 1 (1998): 39–44.

5. J. K. Shen and H. T. Zhang, "Function and Structure of Bradykinin Receptor 2 for Drug Discovery," *Acta Pharmacologica Sinica* 44, no. 3 (2023): 489–498.

6. R. C. Dutra, "Kinin Receptors: Key Regulators of Autoimmunity," *Autoimmunity Reviews* 16, no. 2 (2017): 192–207.

7. A. Nokkari, H. Abou-El-Hassan, Y. Mechref, et al., "Implication of the Kallikrein-Kinin System in Neurological Disorders: Quest for Potential Biomarkers and Mechanisms," *Progress in Neurobiology* 165–167 (2018): 26–50.

8. E. S. M. Rocha, W. T. Beraldo, and G. Rosenfeld, "Bradykinin, a Hypotensive and Smooth Muscle Stimulating Factor Released From Plasma Globulin by Snake Venoms and by Trypsin," *American Journal of Physiology* 156, no. 2 (1949): 261–273.

9. C. M. Costa-Neto, P. Dillenburg-Pilla, T. A. Heinrich, et al., "Participation of Kallikrein-Kinin System in Different Pathologies," *International Immunopharmacology* 8, no. 2 (2008): 135–142.

10. J. F. Hess, J. A. Borkowski, G. S. Young, C. D. Strader, and R. W. Ransom, "Cloning and Pharmacological Characterization of a Human Bradykinin (BK-2) Receptor," *Biochemical and Biophysical Research Communications* 184, no. 1 (1992): 260–268.

11. J. G. Menke, J. A. Borkowski, K. K. Bierilo, et al., "Expression Cloning of a Human B1 Bradykinin Receptor," *Journal of Biological Chemistry* 269, no. 34 (1994): 21583–21586.

12. J. Chao, H. J. Li, Y. Y. Yao, et al., "Kinin Infusion Prevents Renal Inflammation, Apoptosis, and Fibrosis via Inhibition of Oxidative Stress and Mitogen-Activated Protein Kinase Activity," *Hypertension* 49, no. 3 (2007): 490–497.

13. G. Bledsoe, B. Shen, Y. Yao, J. J. Zhang, L. Chao, and J. Chao, "Reversal of Renal Fibrosis, Inflammation, and Glomerular Hypertrophy by Kallikrein Gene Delivery," *Human Gene Therapy* 17, no. 5 (2006): 545–555.

14. M. A. Jaffa, F. Kobeissy, M. Al Hariri, et al., "Global Renal Gene Expression Profiling Analysis in B2-Kinin Receptor Null Mice: Impact of Diabetes," *PLoS One* 7, no. 9 (2012): e44714.

15. M. Kakoki, N. Takahashi, J. C. Jennette, and O. Smithies, "Diabetic Nephropathy Is Markedly Enhanced in Mice Lacking the Bradykinin B2 Receptor," *Proceedings of the National Academy of Sciences of the United States of America* 101, no. 36 (2004): 13302–13305.

16. M. Pouliot, S. Talbot, J. Sénécal, F. Dotigny, E. Vaucher, and R. Couture, "Ocular Application of the Kinin B1 Receptor Antagonist LF22-0542 Inhibits Retinal Inflammation and Oxidative Stress in Streptozotocin-Diabetic Rats," *PLoS One* 7, no. 3 (2012): e33864.

17. M. Abdouh, S. Talbot, R. Couture, and H. M. Hasséssian, "Retinal Plasma Extravasation in Streptozotocin-Diabetic Rats Mediated by Kinin B(1) and B(2) Receptors," *British Journal of Pharmacology* 154, no. 1 (2008): 136–143.

18. S. Delemasure, N. Blaes, C. Richard, et al., "Antioxidant/Oxidant Status and Cardiac Function in Bradykinin B(1)- and B(2)-receptor Null Mice," *Physiological Research* 62, no. 5 (2013): 511–517.

19. M. T. Lemos, F. A. Amaral, K. E. Dong, et al., "Role of Kinin B1 and B2 Receptors in Memory Consolidation During the Aging Process of Mice," *Neuropeptides* 44, no. 2 (2010): 163–168.

20. C. A. Trujillo, P. D. Negraes, T. T. Schwindt, et al., "Kinin-B2 Receptor Activity Determines the Differentiation Fate of Neural Stem Cells," *Journal of Biological Chemistry* 287, no. 53 (2012): 44046–44061.

21. C. F. Xia, H. Yin, Y. Y. Yao, C. V. Borlongan, L. Chao, and J. Chao, "Kallikrein Protects Against Ischemic Stroke by Inhibiting Apoptosis and Inflammation and Promoting Angiogenesis and Neurogenesis," *Human Gene Therapy* 17, no. 2 (2006): 206–219.

22. I. C. Nascimento, T. Glaser, A. A. Nery, M. M. Pillat, J. B. Pesquero, and H. Ulrich, "Kinin-B1 and B2 Receptor Activity in Proliferation and Neural Phenotype Determination of Mouse Embryonic Stem Cells," *Cytometry, Part A* 87, no. 11 (2015): 989–1000.

23. M. M. Pillat, C. Lameu, C. A. Trujillo, et al., "Bradykinin Promotes Neuron-Generating Division of Neural Progenitor Cells Through ERK Activation," *Journal of Cell Science* 129, no. 18 (2016): 3437–3448.

24. F. Wasinski, R. O. Batista, M. Bader, R. C. Araujo, and F. Klempin, "Bradykinin B2 Receptor Is Essential to Running-Induced Cell Proliferation in the Adult Mouse Hippocampus," *Brain Structure & Function* 223, no. 8 (2018): 3901–3907.

25. M. Gröger, D. Lebesgue, D. Pruneau, et al., "Release of Bradykinin and Expression of Kinin B2 Receptors in the Brain: Role for Cell Death and Brain Edema Formation After Focal Cerebral Ischemia in Mice," *Journal of Cerebral Blood Flow and Metabolism* 25, no. 8 (2005): 978–989.

26. J. Do, J. I. Kim, J. Bakes, K. Lee, and B. K. Kaang, "Functional Roles of Neurotransmitters and Neuromodulators in the Dorsal Striatum," *Learning and Memory* 20, no. 1 (2012): 21–28.

27. T. M. Franco, M. R. Tavares, L. S. Novaes, et al., "Effects of Bradykinin B2 Receptor Ablation From Tyrosine Hydroxylase Cells on Behavioral and Motor Aspects in Male and Female Mice," *International Journal of Molecular Sciences* 25, no. 3 (2024): 1490.

28. I. E. de Araujo, A. J. Oliveira-Maia, T. D. Sotnikova, et al., "Food Reward in the Absence of Taste Receptor Signaling," *Neuron* 57, no. 6 (2008): 930–941.

29. A. Buttigieg, O. Flores, A. Hernández, P. Sáez-Briones, H. Burgos, and C. Morgan, "Preference for High-Fat Diet Is Developed by Young Swiss CD1 Mice After Short-Term Feeding and Is Prevented by NMDA Receptor Antagonists," *Neurobiology of Learning and Memory* 107 (2014): 13–18.

30. P. Svenningsson, A. Nishi, G. Fisone, J. A. Girault, A. C. Nairn, and P. Greengard, "DARPP-32: An Integrator of Neurotransmission," *Annual Review of Pharmacology and Toxicology* 44 (2004): 269–296.

31. M. F. Naso, B. Tomkowicz, W. L. Perry, 3rd, and W. R. Strohl, "Adeno-Associated Virus (AAV) as a Vector for Gene Therapy," *BioDrugs* 31, no. 4 (2017): 317–334.

32. I. Duka, E. Kintsurashvili, I. Gavras, C. Johns, M. Bresnahan, and H. Gavras, "Vasoactive Potential of the b(1) Bradykinin Receptor in

Normotension and Hypertension," *Circulation Research* 88, no. 3 (2001): 275–281.

33. L. Luo, M. C. Ambrozkiewicz, F. Benseler, et al., "Optimizing Nervous System-Specific Gene Targeting With Cre Driver Lines: Prevalence of Germline Recombination and Influencing Factors," *Neuron* 106, no. 1 (2020): 37–65.e5.

34. A. Niewiarowska-Sendo, A. Polit, M. Piwowar, M. Tworzydło, A. Kozik, and I. Guevara-Lora, "Bradykinin B2 and Dopamine D2 Receptors Form a Functional Dimer," *Biochimica et Biophysica Acta (BBA) - Molecular Cell Research* 1864, no. 10 (2017): 1855–1866.

35. P. F. Marcott, S. Gong, P. Donthamsetti, et al., "Regional Heterogeneity of D2-Receptor Signaling in the Dorsal Striatum and Nucleus Accumbens," *Neuron* 98, no. 3 (2018): 575–87.e4.

36. X. Zhu, D. Ottenheimer, and R. J. DiLeone, "Activity of D1/2 Receptor Expressing Neurons in the Nucleus Accumbens Regulates Running, Locomotion, and Food Intake," *Frontiers in Behavioral Neuroscience* 10 (2016): 66.

37. W. Han, L. A. Tellez, M. H. Perkins, et al., "A Neural Circuit for Gut-Induced Reward," *Cell* 175, no. 3 (2018): 665–78.e23.

38. M. M. Hagan, P. A. Rushing, L. M. Pritchard, et al., "Long-Term Orexigenic Effects of AgRP-(83–132) Involve Mechanisms Other Than Melanocortin Receptor Blockade," *American Journal of Physiology. Regulatory, Integrative and Comparative Physiology* 279, no. 1 (2000): R47–R52.

39. D. D. Markov, "Sucrose Preference Test as a Measure of Anhedonic Behavior in a Chronic Unpredictable Mild Stress Model of Depression: Outstanding Issues," *Brain Sciences* 12, no. 10 (2022): 1287.

40. M. Y. Liu, C. Y. Yin, L. J. Zhu, et al., "Sucrose Preference Test for Measurement of Stress-Induced Anhedonia in Mice," *Nature Protocols* 13, no. 7 (2018): 1686–1698.

41. S. Gencturk and G. Unal, "Rodent Tests of Depression and Anxiety: Construct Validity and Translational Relevance," *Cognitive, Affective, & Behavioral Neuroscience* 24, no. 2 (2024): 191–224.

42. M. L. Seibenhener and M. C. Wooten, "Use of the Open Field Maze to Measure Locomotor and Anxiety-Like Behavior in Mice," *Journal of Visualized Experiments* 96 (2015): e52434.

43. V. Carola, F. D'Olimpio, E. Brunamonti, F. Mangia, and P. Renzi, "Evaluation of the Elevated Plus-Maze and Open-Field Tests for the Assessment of Anxiety-Related Behaviour in Inbred Mice," *Behavioural Brain Research* 134, no. 1–2 (2002): 49–57.

44. J. D. Mul, "Voluntary Exercise and Depression-Like Behavior in Rodents: Are We Running in the Right Direction?," *Journal of Molecular Endocrinology* 60, no. 3 (2018): R77–r95.

45. E. Binder, S. K. Droste, F. Ohl, and J. M. Reul, "Regular Voluntary Exercise Reduces Anxiety-Related Behaviour and Impulsiveness in Mice," *Behavioural Brain Research* 155, no. 2 (2004): 197–206.

46. C. H. Duman, L. Schlesinger, D. S. Russell, and R. S. Duman, "Voluntary Exercise Produces Antidepressant and Anxiolytic Behavioral Effects in Mice," *Brain Research* 1199 (2008): 148–158.

47. R. L. Albin, A. B. Young, and J. B. Penney, "The Functional Anatomy of Basal Ganglia Disorders," *Trends in Neurosciences* 12, no. 10 (1989): 366–375.

48. C. R. Gerfen, T. M. Engber, L. C. Mahan, et al., "D1 and D2 Dopamine Receptor-Regulated Gene Expression of Striatonigral and Striatopallidal Neurons," *Science* 250, no. 4986 (1990): 1429–1432.

49. A. V. Kravitz, B. S. Freeze, P. R. Parker, et al., "Regulation of Parkinsonian Motor Behaviours by Optogenetic Control of Basal Ganglia Circuitry," *Nature* 466, no. 7306 (2010): 622–626.

50. C. M. Novak, P. R. Burghardt, and J. A. Levine, "The Use of a Running Wheel to Measure Activity in Rodents: Relationship to Energy Balance, General Activity, and Reward," *Neuroscience and Biobehavioral Reviews* 36, no. 3 (2012): 1001–1014.

51. K. C. Berridge, T. E. Robinson, and J. W. Aldridge, "Dissecting Components of Reward: 'liking', 'wanting', and Learning," *Current Opinion in Pharmacology* 9, no. 1 (2009): 65–73.

52. K. C. Berridge and T. E. Robinson, "Liking, Wanting, and the Incentive-Sensitization Theory of Addiction," *American Psychologist* 71, no. 8 (2016): 670–679.

53. P. Greengard, A. C. Nairn, J. A. Girault, et al., "The DARPP-32/Protein Phosphatase-1 Cascade: A Model for Signal Integration," *Brain Research. Brain Research Reviews* 26, no. 2–3 (1998): 274–284.

54. K. C. Langley, C. Bergson, P. Greengard, and C. C. Ouimet, "Co-Localization of the D1 Dopamine Receptor in a Subset of DARPP-32-Containing Neurons in Rat Caudate-Putamen," *Neuroscience* 78, no. 4 (1997): 977–983.

55. G. Gangarossa, J. Espallergues, P. Mailly, et al., "Spatial Distribution of D1R- and D2R-Expressing Medium-Sized Spiny Neurons Differs Along the Rostro-Caudal Axis of the Mouse Dorsal Striatum," *Frontiers in Neural Circuits* 7 (2013): 124.

56. D. J. Surmeier, W. J. Song, and Z. Yan, "Coordinated Expression of Dopamine Receptors in Neostriatal Medium Spiny Neurons," *Journal of Neuroscience* 16, no. 20 (1996): 6579–6591.

Supporting Information

Additional supporting information can be found online in the Supporting Information section. **Figure S1:** Striatal B2R deletion modifies hedonic behavior in the sucrose preference test. Sucrose consumption over a 24-h period normalized by body weight in control (CTL) and $ST^{\Delta B2R}$ mice ($n = 10$ per group). Data are expressed as mean ± SEM. Statistical significance was assessed using Student's *t*-test; $^{*}p < 0.05$. **Figure S2:** Voluntary wheel-running performance in mice with striatal B2R ablation. Daily distance traveled (in kilometers, km) across the 7-day experimental period in control (CTL) and $ST^{\Delta B2R}$ mice ($n = 7$–10 per group). Data are expressed as mean ± SEM. Statistical analysis: Student's *t*-test; $^{*}p < 0.05$; $^{**}p < 0.01$; $^{***}p < 0.001$. **Figure S3:** Lack of co-localization between the dTomato reporter and GFAP or Parvalbumin proteins in the dorsal striatum. (A, B) Representative images showing glial fibrillary acidic protein (GFAP) immunofluorescence (green) and dTomato reporter expression (magenta). (C, D) Representative images showing parvalbumin immunofluorescence (green) and dTomato reporter expression (magenta). Scale bar: 100 μm (left panels) and 200 μm (right panels). LV: lateral ventricle. **Table S1:** Summary of statistical analyzes for all behavioral and metabolic assays.